Inorg. Chem. **2007**, *46*, 10187–10199

Synthesis and Characterization of Iridium(III) Cyclometalated Complexes with Oligonucleotides: Insights into Redox Reactions with DNA

Fangwei Shao, Benjamin Elias, Wei Lu,† and Jacqueline K. Barton*

Division of Chemistry and Chemical Engineering, California Institute of Technology, Pasadena, California 91125

Received July 13, 2007

Heteroleptic cyclometalated complexes of Ir(III) containing the dipyridophenazine ligand are synthesized through the direct introduction of a functionalized dipyridophenazine ligand onto a bis(dichloro)-bridged Ir(III) precusor and characterized by ^{1}H NMR, mass spectrometry, as well as spectroscopic and electrochemical properties. The excited state of the Ir(III) complexes have sufficient driving force to oxidize purines and to reduce pyrimidine nucleobases. Luminescence and EPR measurements of the Ir(III) complex with an unmodified dppz bound to DNA show the formation of a guanine radical upon irradiation, resulting from an oxidative photoinduced electron-transfer process. Evidence is also obtained indirectly for reductive photoinduced electron transfer from the excited complex to the thymine base in DNA. We have also utilized cyclopropylamine-substituted nucleosides as ultrafast kinetic traps to report transient charge occupancy in oligonucleotides when DNA is irradiated in the presence of noncovalently bound complexes. These experiments establish that the derivatized Ir(III) complexes, with photoactivation, can trigger the oxidation of guanine and the reduction of cytosine.

Introduction

Various metallointercalators have been extensively used as pendant photooxidants to probe DNA oxidative chemistry with biochemical and spectroscopic assays.[1−8] In particular, both ruthenium and rhodium polypyridine complexes, such as $[Ru(phen)(bpy')(dppz)]^{2+}$ (dppz = dipyrido[3,2-a:2′,3′-c]phenazine) and $[Rh(phi)_2(bpy')]^{3+}$ (phi = 9,10-phenanthrenequinone diimine), were covalently tethered to DNA strands via the 2,2′-bipyridine modified ancillary ligand (bpy′) and have been shown to initiate DNA-mediated hole transport (HT) upon photoactivation.[9] The distant oxidative damage was determined after the reaction of the thermodynamically favored guanine radical[5] with oxygen and water to form irreversible products.[1] Guanine doublets and triplets are frequently adopted as thermal hole traps, in response to photooxidation from ruthenium and rhodium complexes.[10,11] However, the true mechanism of HT is often obscured by the slow trapping rate of the guanine radical, because multiple electron pathways, such as fast back-electron transfer, occur during the ms lifetime of the guanine radical.[12] To elucidate the mechanism of HT, several fast kinetic hole traps, such as N_2-cyclopropyl-guanine (^{CP}G)[13] and N_4-cyclopropyl-cytosine (^{CP}C)[14] have been developed to probe the transient hole occupancy on bridging bases. Recently, DNA-mediated HT has been investigated extensively by using transition-

* To whom correspondence should be addressed. E-mail: jkbarton@caltech.edu.

† Present Address: Department of Chemistry, The University of Hong Kong, Pokfulam Road, Hong Kong SAR, China.

(1) Hall, D. B.; Holmlin, R. E.; Barton, J. K. *Nature* **1996**, *382*, 731−735.
(2) Núñez, M. E.; Barton, J. K. *Curr. Opin. Chem. Biol.* **2000**, *4*, 199−206.
(3) O'Neill, M. A.; Barton, J. K. *Charge Transfer in DNA: From Mechanism to Application*; Wagenknecht, H. A., Ed.; Wiley & Sons: New York, 2005; pp 27−75.
(4) Friedman, A. E.; Chambron, J. C.; Sauvage, J. P.; Turro, N. J.; Barton, J. K. *J. Am. Chem. Soc.* **1990**, *112*, 4960−4962.
(5) Stemp, E. D. A.; Arkin, M.; Barton, J. K. *J. Am. Chem. Soc.* **1997**, *119*, 2921−2925.
(6) Augustyn, K. E.; Pierre, V. C.; Barton, J. K. *Wiley Encyclopedia Chemical Biology*; 2007; in press.
(7) Yoo, J.; Delaney, S.; Stemp, E. D. A.; Barton, J. K. *J. Am. Chem. Soc.* **2003**, *125*, 6640−6641.
(8) Holmlin, R. E.; Stemp, E. D. A.; Barton, J. K. *J. Am. Chem. Soc.* **1996**, *118*, 5236−5244.
(9) Delaney, S.; Barton, J. K. *J. Org. Chem.* **2003**, *68*, 6475−6483.
(10) Delaney, S.; Yoo, J.; Stemp, E. D. A.; Barton, J. K. *Proc. Nat. Acad. Sci. U.S.A.* **2004**, *101*, 10511−10516.
(11) Núñez, M. E.; Hall, D. B.; Barton, J. K. *Chem. Biol.* **1999**, *6*, 85−97.
(12) (a) Williams, T. T.; Dohno, C.; Stemp, E. D. A.; Barton, J. K. *J. Am. Chem. Soc.* **2004**, *126*, 8148−8158. (b) Dohno, C.; Stemp, E. D. A.; Barton, J. K. *J. Am. Chem. Soc.* **2003**, *125*, 9586−9587.
(13) Nakatani, K.; Dohno, C.; Saito, I. *J. Am. Chem. Soc.* **2001**, *123*, 9681−9682.
(14) Shao, F.; O'Neill, M. A.; Barton, J. K. *Proc. Nat. Acad. Sci. U.S.A.* **2004**, *101*, 17914−17919.

10.1021/ic7014012 CCC: $37.00
Published on Web 10/31/2007

metal complexes as photooxidants and a variety of modified nucleobases as hole traps.[14−17]

DNA-mediated electron transport (ET) is also an electron migration process involving the reduction of DNA bases at a distance.[18] Unlike HT, DNA ET has not been studied extensively in solution, partially because of the lack of proper photoreductants with close interaction toward DNA, as well as efficient electron traps. DNA-mediated ET has been explored electrochemically using DNA films, but here the focus has been on sensor development.[19] Long-range reductive chemistry on DNA in solution has been demonstrated but only using organic reductants such as flavin or aromatic amines.[20−24] These reductants adopt different interaction modes with the double helix compared to the metallointercalating photooxidants. Common electron traps often used for ET studies involve cyclobutane pyrimidine dimers[23] or cyclopropyl-modified nucleobases (such as ^{CP}C).[25] Both systems are known to undergo a ring-opening reaction upon one-electron oxidation or reduction and can thus monitor efficiently transient electron occupancy over nucleobases.

DNA-mediated ET and HT have thus been investigated using different photoredox probes and traps. The coupling of the photoredox probe into the DNA base stack is, however, crucial for the DNA-mediated charge migration process.[26] Therefore, we were interested in studying both ET and HT with a unique photoredox probe well coupled to DNA containing cyclopropylamine-substituted nucleobases to probe both oxidative or reductive processes on a picosecond time scale.[14] Metal complexes with an intercalative ligand and suitable redox properties could thus be good candidates. Recently, a series of water-soluble platinum complexes with the dppz ligand have been developed in our group.[25] $[(mes)_2Pt(dppz)]^{2+}$ (mes = *N*,*N*,*N*,3,5-pentamethylaniline) can simultaneously promote oxidatively the ring-opening reaction of ^{CP}G and reductively decompose ^{CP}C in DNA. However, these platinum complexes are difficult to functionalize and covalently tether to DNA strands, making the parallel study of DNA-mediated ET and HT untenable.

Cyclometalated Ir(III) complexes are well-known to be stable upon irradiation and have been extensively applied in the design and preparation of light-emitting diodes.[27−29] Recently, Ir(III) diimine complexes have also been developed as luminescent labels for biological applications.[30,31] More specifically, positively charged $[Ir(ppy)_2(dppz)]^+$ (ppy = 2-phenylpyridine) has shown luminescence and avid DNA binding.[32] With proper design of ancillary and intercalative diimine ligands, Ir(III) cyclometalated complexes would be able to trigger oxidative or reductive damage in DNA upon photolysis. Moreover, it is possible to introduce a monofunctional linkage to the iridium complex through modification of the diimine moiety, allowing further conjugation to DNA strands.[25,32]

Here, we report the synthesis and photochemistry of three novel Ir(III) complexes with a functionalized dppz ligand. On the basis of the spectroscopic and electrochemical data, oxidation of purine or reduction of pyrimidine nucleobases can be initiated upon irradiation with these Ir(III) complexes. The redox chemistry of DNA has been revealed by both spectroscopic and fast ring-opening chemistry of modified nucleobases. The work represents the foundation for studies of long-range photoreduction on DNA with covalently tethered analogues.[33] These results confirm the power of Ir(III) complexes in the study of HT/ET chemistry within DNA.

Experimental Section

Materials. 1,10-phenanthroline-5,6-dione (phendione),[34] dipyrido[3,2-a:2′,3′-c]phenazine,[34] cyclometalated Ir(III) μ-dichloro-bridged dimer ($[Ir(ppy)_2Cl]_2$, ppy: 2-phenylpyridine),[35] and ethylhex-5-ynoate[36] were synthesized as described previously. All of the solvents and reagents for the synthesis were at least of reagent grade and were used without further purification. All of the solvents for the spectroscopic and electrochemical measurements were of spectroscopic grade. Calf thymus DNA (CT-DNA, Pharmacia) was purified by exhaustive dialysis against a phosphate buffer solution (pH 7) and subsequently against water. *Clostridium Perfringens* DNA (CP-DNA, Sigma) and Herring testes DNA (HT-DNA, Sigma) were purified by exhaustive dialysis against a TRIS-HCl buffer solution (pH 7.4) and afterward against water. $[Poly(dA-dT)]_2$, $[poly(dG-dC)]_2$ (Pharmacia, GE Healthcare) and λ DNA

(15) O'Neill, M. A.; Barton, J. K. *J. Am. Chem. Soc.* **2004**, *126*, 11471−11483.
(16) Shao, F.; Augustyn, K. E.; Barton, J. K. *J. Am. Chem. Soc.* **2005**, *127*, 17445−17452.
(17) Augustyn, K. E.; Genereux, J. C.; Barton, J. K. *Angew. Chem., Int. Ed.* **2007**, *46*, 5731−5733.
(18) (a) Behrens, C.; Cichon, M. K.; Grolle, F.; Hennecke, U.; Carell, T. *Top. Curr. Chem.* **2004**, *236*, 187−204. (b) Wagenknecht, H.-A. *Angew. Chem., Int. Ed.* **2003**, *42*, 2454−2460.
(19) (a) Kelley, S. O.; Jackson, N. M.; Hill, M. G.; Barton, J. K. *Angew. Chem., Int. Ed.* **1999**, *38*, 941−945. (b) Boon, E. M.; Drummond, T. G.; Hill, M. G.; Barton, J. K. *Nature Biotech.* **2000**, *18*, 1096−1100.
(20) Breeger, S.; Hennecke, U.; Carell, T. *J. Am. Chem. Soc.* **2004**, *126*, 1302−1303.
(21) Lewis, F. D.; Liu, X.; Miller, S. E.; Hayes, R. T.; Wasielewski, M. R. *J. Am. Chem. Soc.* **2002**, *124*, 11280−11281.
(22) (a) Ito, T.; Rokita, S. E. *J. Am. Chem. Soc.* **2004**, *126*, 15552−15559. (b) Ito, T.; Rokita, S. E. *J. Am. Chem. Soc.* **2003**, *125*, 11480−11481. (c) Ito, T.; Rokita, S. E. *Angew. Chem., Int. Ed.* **2004**, *43*, 1839−1842.
(23) (a) Giese, B.; Carl, B.; Carl, T.; Carell, T.; Behrens, C.; Hennecke, U.; Schieman, O.; Feresin, E. *Angew. Chem., Int. Ed.* **2004**, *43*, 1848−1851. (b) Schwögler, A.; Burgdorf, L. T.; Carell, T. *Angew. Chem., Int. Ed.* **2000**, *39*, 3918−3920.
(24) (a) Breeger, S.; Hennecke, U.; Carell, T. *J. Am. Chem. Soc.* **2004**, *126*, 1302−1303. (b) Manetto, A.; Breeger, S.; Chatgilialoglu, C.; Carell, T. *Angew. Chem., Int. Ed.* **2006**, *45*, 318−321.
(25) Lu, W.; Vicic, D. A.; Barton, J. K. *Inorg. Chem.* **2005**, *44*, 7970−7980.
(26) Kelley, S. O.; Barton, J. K. *Science*, **1999**, *283*, 375−381.
(27) Tamayo, A. B.; Simona, G.; Sajoto, T.; Djurovich, P. I.; Tsyba, I. M.; Bau, R.; Thompson, M. E. *Inorg. Chem.* **2005**, *44*, 8723−8732.
(28) Lamansky, S.; Djurovich, P.; Murphy, D.; Abdel-Razzaq, F.; Lee, H.; Adachi, C.; Burrows, P. E.; Forrest, S. R.; Thompson, M. E. *J. Am. Chem. Soc.* **2001**, *123*, 4304−4312.
(29) Lepeltier, M.; Lee, T. K.; Lo, K. K.; Toupet, L.; Bozec, H. L.; Guerchais, V. *Eur. J. Inorg. Chem.* **2005**, 110−117.
(30) Lo, K. K.; Ng, D. C.; Chung, C. *Organometallics* **2001**, *20*, 4999−5001.
(31) Lo, K. K.; Chung, C.; Lee, T. K.; Lui, L.; Tsang, K. H.; Zhu, N. *Inorg. Chem.* **2003**, *42*, 6886−6897.
(32) Lo, K. K.; Chung, C.; Zhu, N. *Chem.—Eur. J.* **2006**, *12*, 1500−1512.
(33) Shao, F.; Barton, J. K. *J. Am. Chem. Soc.*, in press.
(34) Dupureur, C. M.; Barton, J. K. *Inorg. Chem.* **1997**, *36*, 33−43.
(35) Lamansky, S.; Djurovich, P.; Murphy, D.; Abdel-Razzaq, F.; Kwong, R.; Tsyba, I.; Bortz, M.; Mui, B.; Bau, R.; Thompson, M. E. *Inorg. Chem.* **2001**, *40*, 1704−1711.
(36) Duclos, S.; Stoeckli-Evans, H.; Ward, T. R. *Helv. Chim. Acta* **2001**, *84*, 3148−3161.

(Hind III fragments, Invitrogen, 0.5 μg/μl) were used as received. Polynucleotide phosphate concentrations were determined spectrophotometrically ($\epsilon_{260\ nm} = 6600\ M^{-1}\ cm^{-1}$ for CT-DNA, HT-DNA, and CP-DNA;[37] $\epsilon_{262\ nm} = 6600\ M^{-1}\ cm^{-1}$ for [Poly(dA-dT)]$_2$;[38] $\epsilon_{254\ nm} = 8400\ M^{-1}\ cm^{-1}$ for [Poly(dG-dC)]$_2$).[39]

Instrumentation. ^{1}H NMR (300 MHz) spectra were obtained on a Bruker Avance-300 instrument. The chemical shifts were measured versus the solvent as an internal standard. Absorption spectra were recorded on a Beckman DU 7400 spectrophotometer. The molar absorption coefficients were determined by weight and absorption measurements. Emission spectra were recorded with an ISS K2 fluorimeter (5 mm path length) equipped with a Peltier-controlled thermostated sample holder (Quantum Northwest) and a 250 W xenon lamp as excitation source. The samples were excited at the maximum of the lowest absorption band for each complex. Excitation spectra were monitored at the emission maximum for excitation wavelength between 300 and 550 nm. Reversed phase HPLC was carried out with an HP 1050 or HP 1100 system on a Dynamax 300 Å C_{18} column (Varian).

Cyclic voltammetry was performed in a one-compartment cell, using a glassy carbon disk working electrode (approximate area = 0.03 cm^2), a platinum counter-electrode, and Ag/AgCl as a reference electrode. The potential applied to the working electrode was controlled by a Bioanalytical Systems model CV-50W electrochemical analyzer. Scan rates of 100 mV s^{-1} between -1.5 and $+1.6$ V versus the reference electrode were used. The voltammograms were recorded with dry acetonitrile solutions (Fluka, stored over molecular sieves). The concentration of the complexes was 800 μM, with 0.1 mol/L tetrabutylammonium hexafluorophosphate as the supporting electrolyte. Before each measurement, the samples were purged using argon. $E_{1/2}$ values were obtained from the average of E measured at the maximum peak current intensity for the forward and reverse electrochemical processes. Potentials were adjusted to NHE, using the oxidation of ferrocene as an internal standard.

EPR spectra were recorded on a continuous-wave X-band EPR spectrometer (EMX, Bruker). The light source used was a 250 W xenon lamp. The light was passed through a filter ($\lambda > 350$ nm) and focused on the sample with an optic fiber. Spectra were recorded at ambient temperature after 90 s irradiation.

Preparations and Photoredox Reactions of DNA Oligonucleotides. Unmodified DNA oligonucleotides were synthesized by standard phosphoramidite chemistry on an ABI 392 DNA/RNA synthesizer. Cyclopropylamine-modified DNA assemblies were synthesized and purified as described previously.[14] The photoredox reactions of Ir(III) complexes with modified oligonucleotides were carried out aerobically, unless otherwise stated. Anaerobic samples were obtained using the freeze−pump−thaw method in airtight cuvettes under argon. The samples were irradiated with a 1000 W Hg−Xe lamp ($\lambda_{irradiation} = 380$ nm) equipped with a 320 nm long pass filter. After irradiation, oligonucleotides were digested by 37 °C incubation with phosphodiesterase (USB), and alkaline phosphatase (Roche) for 24 h to yield nucleosides. After incubation, RP-HPLC (Chemcobond 5-ODS−H, 4.6 × 100 mm, 2% MeCN/98% 50 mM NH_4OAc ~12% MeCN/ 88% 50 mM NH_4OAc over 30 min) was applied to analyze the decomposition products of cyclopropylamine-modified nucleosides. The percentage of modified deoxynucleobase decomposition was determined by subtracting the ratio of the area under the peak of the undecomposed modified deoxynucleobase in an irradiated sample over that in a nonirradiated sample (dark control) from one, with adenine or inosine as an internal standard for all of the HPLC traces. Irradiations were repeated three times, and the results were averaged.

Synthetic Procedures and Characterization. The synthesis of the Ir(III) cyclometalated dppz complexes involves the chelation of a modified or unmodified dppz on a μ-dichloro-bridged precursor [Ir(ppy)$_2$Cl]$_2$. All of the reaction mixtures were protected from direct light during the synthesis to prevent photochemical degradation, and the reactions were conducted under argon. After synthesis and purification, the compounds were characterized by ^{1}H NMR spectroscopy (300 MHz) and by MALDI-MS unless otherwise indicated. All of the multiplicity and coupling constants could not be determined due to the superposition of several signals and/or lack of fine resolution for some peaks in the ^{1}H NMR spectra.

For the sake of clarity, the following abbreviations for the different derivatives (Figure 1) are used throughout: **dppz0** for unmodified dppz ligand, **dppz1** for methyl dipyrido[3,2-a:2′,3′-c]-phenazine-11-oxy-hex-5-ynoate, **dppz2** for ethyl dipyrido[3,2-a:2′,3′-c]phenazine-11-zoate, **dppz3** for ethyl (dipyrido[3,2-a:2′,3′-c]phenazine-11-yl)-hex-5-ynoate; **Ir0** for [Ir(ppy)$_2$dppz]$^+$, **Ir1** for [Ir(ppy)$_2$**dppz1**]$^+$, **Ir2** for [Ir(ppy)$_2$**dppz2**]$^+$, and **Ir3** for [Ir(ppy)$_2$**dppz3**]$^+$.

Synthesis of Derivatized dppz Ligands (Figure 1). dppz1. Methyl 6-Iodohexanoate (1). ϵ-caprolactone (2.28 g, 20 mmol) was added dropwise to 20 mL of a CH_2Cl_2 argon-purged solution containing BF_3 (1.0 M), NaI (4.98 g, 30 mmol), and n-Bu_4NI (40 mg, 0.1 mmol). The resulting suspension was stirred at ambient temperature for 16 h, and the reaction was quenched afterward with anhydrous MeOH (5 mL). The solution was diluted up to 70 mL with CH_2Cl_2 and washed thoroughly with aqueous $NaHCO_3$ (50 mL), $Na_2S_2O_3$ (50 mL), and water (50 mL). The organic phase was dried over anhydrous $MgSO_4$ and evaporated to yield a brownish oil. Percolation through a short silica gel column with hexane yielded pure **1** (colorless oil).

Methyl 6-(3-Amino-4-nitrophenoxy)hexanoate (2). A mixture of 4-amino-3-nitrophenol (0.52 g, 3.4 mmol) and NaH (60% in mineral oil, 136 mg, 5.7 mmol) in anhydrous DMF (20 mL) was stirred at room temperature for 15 min under argon. **1** (0.87 g, 3.4 mmol) was added to the mixture. After 5 h of stirring at room temperature, the solvent was removed under reduced pressure. The crude product was then purified by neutral alumina chromatography (eluant: EtOAc/hexane 1:5, v/v) and yielded the desired product (bright-red solid). Yield: 90%. ^{1}H NMR (300 MHz, $CDCl_3$): δ 7.51 (d, 1H, $J = 2.7$ Hz), 7.03 (dd, 1H, $J = 2.7$ Hz, $J = 9.3$ Hz), 6.75 (d, 1H, $J = 9.3$ Hz), 5.90 (broad s, 2H), 3.91 (t, 2H, $J = 9.3$ Hz), 3.67 (s, 3H), 2.34 (t, 2H, $J = 7.8$ Hz), 1.80~1.72 (m, 2H), 1.70~1.65 (m, 2H), 1.51~1.48 (m, 2H). FAB+: Calcd 282.1216 for $C_{13}H_{18}N_2O_5$, found 282.1214 (M^+).

Methyl 6-(3,4-Diaminophenoxy)hexanoate and dppz1 (3). Palladium carbon (10% loaded, 0.26 g) was slowly added to a solution of **2** (1.0 g, 13 mmol) in MeOH (40 mL). The mixture was stirred at room temperature for 3 h under H_2 atmosphere. After the complete disappearance of the starting material (TLC, alumina, eluant: EtOAc/hexane 1:5, v/v), the medium was filtered through a short Celite plug into a suspension of 1,10-phenanthroline-5,6-dione (0.75 g, 3.6 mmol) in absolute EtOH (40 mL). After 12 h of refluxing under argon, the reaction mixture was evaporated to dryness. The resulting deep-colored solid was purified with a neutral alumina column (eluant: $CH_3CN/CH_2Cl_2/MeOH = 10:10:1$, v/v/v), sonicated for 30 s in 2 mL acetone, and finally filtered by suction. A further wash with a small portion of acetone yielded a

(37) DelGuerzo, A.; Kirsch − De Mesmaeker, A. *Inorg. Chem.* **2002**, *41*, 938−945.
(38) Inman, R. B.; Baldwin, R. L. *J. Mol. Biol.* **1962**, *5*, 172.
(39) Wells, R. D.; Larson, J. E.; Grant, R. C.; Shortle, B. E.; Cantor, C. R. *J. Mol. Biol.* **1970**, *54*, 465−497.

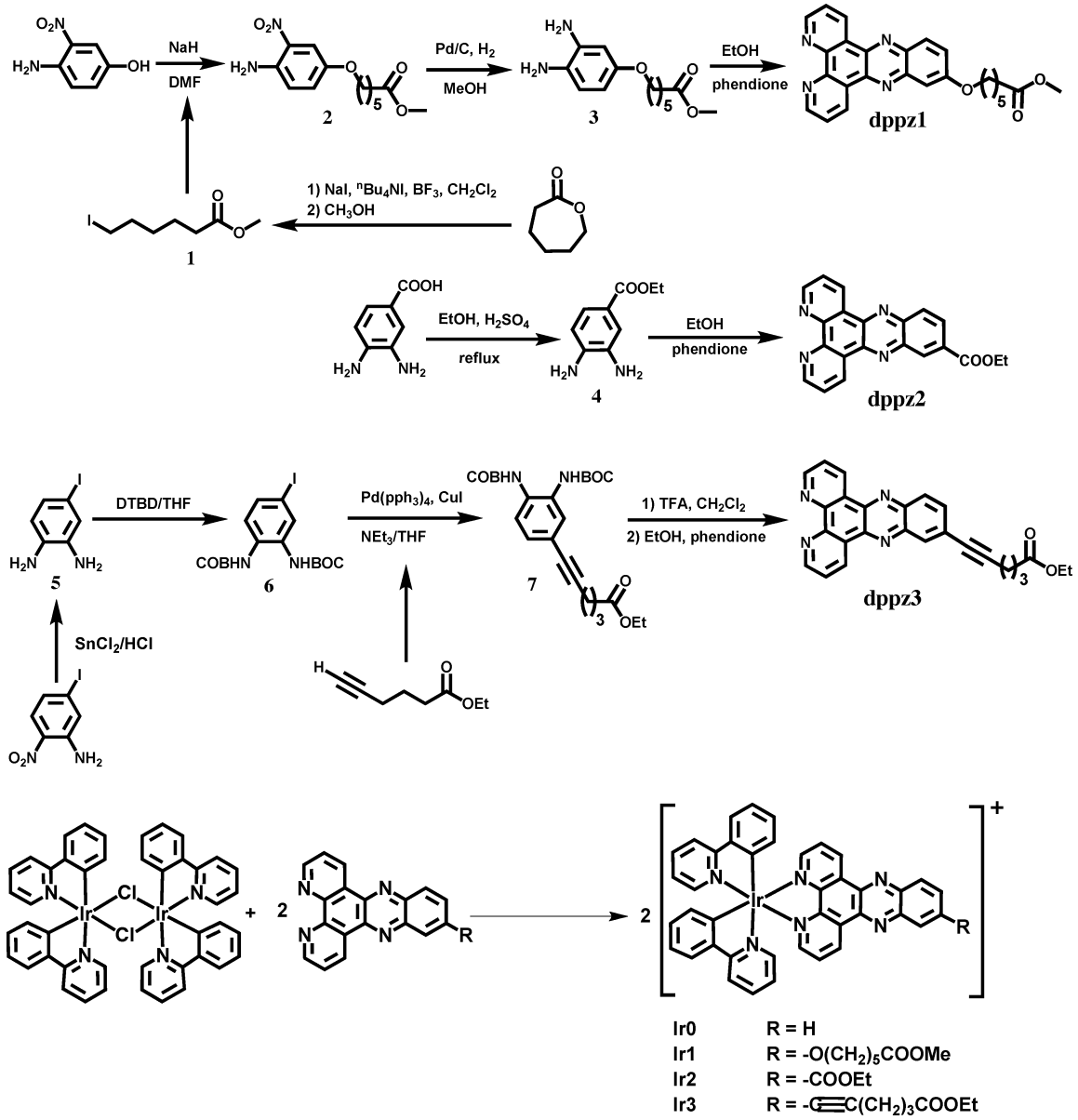

Figure 1. Synthetic route and structures of the four Ir(III) cyclometalated complexes (**Ir0**, **Ir1**, **Ir2**, and **Ir3**) described in this work.

brownish solid (33%). ^{1}H NMR (300 MHz, $CDCl_3$): δ 9.56∼9.52 (m, 2H), 9.26 ∼ 9.21 (m, 2H), 8.16 (d, 1H, J = 9.3 Hz), 7.78 ∼ 7.73 (m, 2H), 7.55∼7.49 (m, 2H), 4.22 (t, 2H, J = 6.3 Hz), 3.69 (s, 3H), 2.43 (t, 2H, J = 7.2 Hz), 1.99∼1.94 (m, 2H), 1.81∼1.76 (m, 2H), 1.63∼1.61 (m). FAB+: Calcd 427.1770 for $C_{25}H_{23}N_4O_3$, found 427.1756 (M^+).

dppz2. Ethyl 3,4-Diaminobenzoate (4). Concentrated sulfuric acid (1 mL) was added dropwise to a suspension of 3,4-diaminobenzoic acid (500 mg, 3.3 mmol) in 30 mL boiling ethanol. After 4 h refluxing, solvent was removed under vacuum. Crude product was dissolved in 30 mL water, and the pH was adjusted to 10 by addition of 1M NaOH. After extraction of the aqueous phase by $CHCl_3$ and subsequent washing of the organic layer with brine and water, evaporation of the chloroform yielded a yellow solid. This latter was used without further purification in the next synthetic step.

dppz2. A warm 10 mL EtOH solution of **4** (0.11 g, 0.6 mmol) was added dropwise to 5 mL boiling EtOH of 1,10-phenanthroline-5,6-dione (0.115 g). Brownish precipitate came out during mixing process. The mixture was refluxed for 10 min. The crude product, collected by suction, was used without further purification. ^{1}H NMR (300 MHz, $CDCl_3$): δ 9.69 (d, 2H, J = 8.1 Hz), 9.34∼9.32 (m, 2H), 9.11 (s, 1H), 8.53 (d, 1H, J = 7.2 Hz), 8.43 (d, 1H, J = 8.1 Hz) 7.86 (m, 2H), 4.55 (q, 2H, J = 7.5 Hz), 1.52 (t, 3H, J = 7.2 Hz). ESI: Calcd 354.1 for $C_{21}H_{14}N_4O_2$, found 355.0 (M^+).

dppz3. 4-Iodobenzene-1,2-diamine (5). 5-iodo-2-nitroaniline (2.64 g, 10 mmol) and $SnCl_2$ (17 g, 90 mmol) were dissolved in 347 mL of concentrated HCl. The reaction mixture was stirred under argon at 70 °C for 4 h and monitored by TLC (Alumina, EtOAc/Hexanes, 1:1, v/v). After the reaction was complete, neutralization of the solution with saturated aqueous Na_2CO_3 yielded color changes (yellow to brown) and precipitates. After extraction of the aqueous phase with ethyl acetate and diethyl ether and a subsequent wash of the organic layer with brine (two times) and drying over anhydrous $MgSO_4$, the removal of the solvent under vacuum yielded crude product, which was immediately used in next step without further purification.

***t*-Butyl-4-iodo-1,2-phenylenedicarbamate (6). 5** (∼10 mmol) and 6.54 g (30 mmol) ditertbutyldicarbonate were dissolved in 50 mL THF and stirred under argon at room temperature overnight.

Extra sodium bicarbonate was added during the reaction to complete the protection of amine groups. The crude product was purified by neutral alumina column (eluant: EtOAc/hexanes, 22/78 v/v). Yield: 70%. ^{1}H NMR (300 Hz, DMSO-d_6): δ 8.59 (s, 2H), 7.85 (s, 1H), 7.37 (d, 1H, J = 10.5 Hz), 7.29 (d, 1H, J = 8.7 Hz) 1,45 (s, 18H). ESI: Calcd 434.1 for $C_{16}H_{23}IN_2O_4$, found 435.0 (M^+).

Ethyl 6-(3,4-Bis(tert-butoxycarbonylamino)phenyl)hex-5-ynoate (7). 6 (260 mg, 0.6 mmol) was mixed with $Pd[P(C_6H_5)_3]_4$ (36 mg, 0.04 mmol) and CuI (14 mg, 0.08mmol) in a dry 25 mL two-neck round-bottom flask under argon. Anhydrous THF (7.5 mL) was added to dissolve the reaction mixture, followed by 450 μL anhydrous triethylamine. Ethyl hex-5-ynoate **(**126 mg, 0.9 mmol) was added to the reaction solution dropwise. After completion (TLC Alumina, EtOAc/hexanes, 1:4, v/v), the isolated product was purified through a silica column (EtOAc/hexanes 28:72, v/v). Yield: 65%. ^{1}H NMR (300 Hz, CD_2Cl_2): δ 7.50∼7.32 (m, 2H), 7.08 (d, 1H, J = 8.6 Hz), 6.71 (broad s, 1H), 6.59 (broad s, 1H), 4.04 (q, 2H, J = 7.2 Hz), 2.48∼2.29 (m, 4H), 1.90∼1.74 (m, 2H), 1.43 (s, 18H), 1.17 (t, 3H, J = 7.2 Hz). FAB+: Calcd 446.2417 for $C_{24}H_{34}N_2O_6$, found 446.2439.

dppz3. 7 (1 g, 2.2 mmol) was dissolved in 20 mL anhydrous dichloromethane under argon. Fifty equiv of anhydrous trifluoroacetic acid was added slowly to the solution. After 1.5 h of stirring at room temperature, the solvent was removed (rotavapor) to yield a deep-brown oil. After neutralization with saturated aqueous Na_2CO_3 and further extraction with ethyl acetate, the oil was added to 0.8 equiv of 1,10-phenanthroline-5,6-dione and dissolved in 7 mL boiling EtOH. The reaction mixture was refluxed for about 2 h. After removal of the solvent under reduced pressure, the crude product was purified through neutral alumina column (2% MeOH/CH_2Cl_2). Yield: 40%. ^{1}H NMR (300 Hz, $CDCl_3$): δ 9.64∼9.62 (d, 2H, J = 10.5 Hz), 9.29∼9.22 (m, 2H), 8.38∼8.24 (m, 2H), 7.89∼7.71 (m, 3H), 4.18 (q, 2H, J = 7.2 Hz), 2.66∼2.56 (m, 4H), 2.11∼1.94 (m, 2H), 1.29 (t, 3H, J = 7.2 Hz). FAB+: Calcd 421.1664 for $C_{26}H_{21}N_4O_2$, found 421.1678.

Synthesis of Ir(III) Cyclometalated Complex with Unfunctionalized dppz (Ir0). One equiv of μ-dichloro-bridged precursor $[Ir(ppy)_2Cl]_2$ (178 mg, 0.166 mmol) was mixed with 2.5 equiv of unfunctionalized dppz (116 mg, 0.409 mmol) and NH_4PF_6 (40 mg, 2.5 mmol) in a solution of 20 mL CH_3CN and 5 mL EtOH. The medium was refluxed, and the reaction was followed by absorption spectroscopy and TLC (silica, eluant CH_3CN/ H_2O/saturated aqueous NH_4Cl 4:5:1). After 14 h, the medium was concentrated, and the addition of small portions of NH_4PF_6 and drops of water yielded orange precipitates. After centrifugation, the solid was washed with excess water, EtOH, and finally dried with ether. RP-HPLC was used for purification of the crude complex (C_{18} column, gradient 45% CH_3CN/55% H_2O/ 83% CH_3CN/17% H_2O over 28 min, both MeCN and H_2O contain 0.1% TFA). The chloride salt was obtained by shaking the complex overnight in an excess of anion exchange resin (sephadex QAE-A25) in water followed by subsequent filtration. ^{1}H NMR (PF_6 salt, 300 MHz, $CDCl_3$): δ 9.79 (dd, 1H, J_1 = 8.1 Hz, J_2 = 1.5 Hz), 8.50 (dd, 1H, J_1 = 6.6 Hz, J_2 = 3.3 Hz), 8.42 (dd, 1H, J_1 = 5.1 Hz, J_2 = 1.5 Hz), 8.16 (dd, 1H, J_1 = 6.6 Hz, J_2 = 3.3 Hz), 8.11 (m, 1H), 8.03 (dd, 1H, J_1 = 8.4 Hz, J_2 = 5.4 Hz), 7.86 (m, 2H), 7.62 (m, 1H), 7.13 (td, 1H, J_1 = 7.5 Hz, J_2 = 1.2 Hz), 7.01 (td, 1H, J_1 = 7.5 Hz, J_2 = 1.2 Hz), 6.93 (td, 1H, J_1 = 6.6 Hz, J_2 = 1.5 Hz), 6.42 (m, 1H). ESI: Calcd 782.9 for $C_{40}H_{24}IrN_6$, found 783.0 (M^+).

Synthesis of Ir(III) Cyclometalated Complexes with Functionalized dppz Ligands. The general synthetic route for functionalized Ir(III) cyclometalated complexes is described in Figure 1. Briefly, 1 equiv of $[Ir(ppy)_2Cl]_2$ and 2 equiv of functionalized dppz were suspended in 15 mL 1:1 MeCN/$CHCl_3$ under argon. After refluxing overnight, evaporation of the solvent under reduced pressure yielded red solids. The precipitates were dissolved in a small amount of $CHCl_3$ and were filtered through a short silica column. A redish-orange band was eluted by 1:1 MeCN/0.4N KNO_3. Afterward, the organic solvent was removed under vacuum, and the precipitate was collected by filtration and redissolved in $CHCl_3$. The solution was dried over $MgSO_4$, and the solvent was removed under vacuum. RP-HPLC (C_{18} column, 45% MeCN/55% H_2O ∼ 80% MeCN/20% H_2O over 30 min, both MeCN and H_2O contain 5% TFA) was used for purification. Chloride salts were obtained from anion exchange chromatography (Sephadex QAE A-25).

[Ir(ppy)$_2$(dppz1)]Cl (Ir1). ^{1}H NMR (300 MHz, $CDCl_3$): δ 9.82 (d, 1H, J = 8.1 Hz), 9.77 (d, 1H, J = 8.4 Hz), 8.35∼8.24 (m, 3H), 7.94∼7.10 (m, 4H), 7.72∼7.70 (m, 4H), 7.65∼7.26 (m, 4H), 7.11∼7.06 (m, 2H), 7.00∼6.98 (m, 4H), 6.41 (d, 2H, J = 7.5 Hz), 4.26 (t, 2H, J = 6.0 Hz), 3.69 (s, 3H), 2.41 (t, 2H, J = 7.2 Hz), 1.97 (m, 2H), 1.77 (m, 2H), 1.61 (m, 2H). FAB+: Calcd 927.2635 for $C_{47}H_{38}IrN_6O_3$, found 927.2607 (M^+).

[Ir(ppy)$_2$(dppz2)]Cl (Ir2). ^{1}H NMR (300 MHz, $CDCl_3$): δ 9.87∼9.83 (m, 2H), 9.12 (d, 1H, J = 2.1 Hz), 8.58∼8.55 (m, 1H), 8.46 (d, 1H, J = 8.7 Hz), 8.38∼8.37 (m, 2H), 8.04∼7.99 (m, 2H), 7.93 (d, 2H, J = 7.8 Hz), 7.75∼7.65 (m, 6H), 7.09 (t, 2H, 7.2 Hz), 7.03∼6.96 (m, 4H), 6.41 (d, 2H, J = 7.2 Hz), 4.54 (q, 2H, J = 7.2 Hz), 1.51 (t, 3H, J = 7.2 Hz). FAB+: Calcd 855.2059 for $C_{43}H_{30}IrN_6O_2$, found 855.2090.

[Ir(ppy)$_2$(dppz3)]Cl (Ir3). ^{1}H NMR (300 MHz, CD_2Cl_2): δ 9.83 (d, 2H, J = 8.4 Hz), 8.48∼8.37 (m, 4H), 8.04∼7.96 (m, 5H), 7.82∼7.74 (m, 4H), 7.49 (d, 2H, J = 4.8 Hz), 7.15 (t, 2H, J = 7.5 Hz), 7.05∼7.00 (m, 2H), 6.89 (t, 2H, J = 7.5 Hz), 6.43 (d, 2H, J = 7.5 Hz), 4.14 (q, 2H, J = 7.2 Hz), 2.64 (t, 2H, J = 7.2 Hz), 2.55 (t, 2H, J = 7.5 Hz), 2.01 (t, 2H, J = 7.5 Hz), 1.26 (t, 3H, J = 7.2 Hz). FAB+: Calcd 921.2529 for $C_{48}H_{36}IrN_6O_2$, found 921.2521.

Results

Synthesis and Characterization. The cyclometalated Ir(III) dppz complexes were synthesized by the direct chelation of either a modified or nonmodified dppz ligand to an iridium dichloro-bridged precursor (Figure 1) using methodologies developed previously for analogous compounds.[29,35,40] The complexes were characterized by MS and by ^{1}H NMR spectroscopy (Experimental Section). The ^{1}H NMR shows unambiguously the presence of a C_2 symmetry axis for the **Ir0**, which induces the equivalence of (i) the proton on the dppz ligand by pairs and (ii) the ancillary ppy ligands. In contrast, **Ir1**, **Ir2**, and **Ir3** do not display any symmetry features as is clearly shown from the analysis of the NMR data. Interestingly, only small differences appear between the chemical shifts of the nonsubstituted Ir(III) complex (**Ir0**) and the substituted ones. Not surprisingly, in the same solvent, the most pronounced effect occurs at the terminal position of the dppz ligand, thus close to the anchoring site, going from a $\Delta\delta$ of ca. −0.3 ppm for **Ir1** (shielding effect of the ether function) to a $\Delta\delta$ of ca. +0.1 ppm for **Ir2** (deshielding effect of the carbonyl group) compared to **Ir0**.

Absorption and Emission Spectroscopy. The absorption and emission data at ambient temperature in different solvents

(40) Didier, P.; Ortmans, I.; Kirsch − De Mesmaeker, A.; Watts, R. J. *Inorg. Chem.* **1993**, *32*, 5239−5245.

Table 1. Absorption, Emission, and Electrochemical Data for the Ir(III) Complexes

feature		Ir0	Ir1	Ir2	Ir3
optical spectra					
absorption[a]		270, 7.12	290, 12.6	278, 10.5	292, 9.46
(λ_{max}^{nm}, ϵ *10^{-4} $M^{-1}cm^{-1}$)		360, 1.86	388, 2.23	369, 1.74	385, 2.56
		382, 1.81	406, 2.53	389, 1.57	405, 3.06
Emission (λ_{max}^{nm})[b]					
−DNA[c]	CH_2Cl_2	628	600	676	634
	MeCN	634	620	Q[d]	715
	Buffer[e]	640	Q	Q	Q
+ DNA	Buffer	Q	N/A	N/A	Q
Electrochemistry (V/NHE)[f]					
E_{ox}		1.5	1.5	1.5	1.5
E_{red}		−0.7	−0.9	−0.6	−0.7
E_{red}^{*}		1.5	1.6	1.8	1.7
E_{ox}^{*}		−0.9	−1.0	−0.9	−0.9

[a] Uncertainty of ϵ is <3%. [b] Excitation wavelength: 375 nm for **Ir0**, 373 nm for **Ir1**, 412 nm for **Ir2**, and 410 nm for **Ir3**. [c] Emission spectra of iridium complexes in the absence (−DNA) and presence (+DNA) of DNA are measured in the solvents indicated in the right column. [d] Luminescence of the iridium complex is quenched under the indicated conditions. [e] Buffer condition: 10 mM NaCl, 20 mM sodium phosphate, pH 7.0. [f] The error associated with the measurements of the redox potentials is estimated to be less than 0.1 V.

under air for each Ir(III) complex are listed in Table 1. Figure 2 and Figure S1 (Supporting Information) show the optical spectra for **Ir0**, **Ir1**, **Ir2**, and **Ir3**. Each compound displays several broad intense absorption bands in the UV−vis region. These bands can be assigned to ligand centered (LC) transitions and to metal-to-ligand charge-transfer (MLCT) transitions Ir → L, where L = ppy or dppz. Indeed, the absorption of complexes made with Ir(III) generally corresponds to the superposition of a different transition involving either the ligands or both the metal and the ligand.[41−43] Interestingly, upon modification of the dppz ligand, shifts are observed for the absorption bands. A common feature at ca. 385 nm remains in all of the spectra, and the low-energy absorption bands are red-shifted in **Ir1** and **Ir3**.

All of the complexes emit strongly in dichloromethane and display one emission maximum, independent of the excitation wavelength. Upon substitution of the dppz ligand, the emission is hypsochromically shifted for **Ir1** ($\lambda_{max,\ em}$ = 600 nm), whereas it is bathochromically shifted for **Ir2** ($\lambda_{max,\ em}$ = 676 nm). Interestingly, the complexes display an important solvatochromic effect, that is, the luminescence is shifted to the red when using more-polar solvents. This shows that the luminescent excited state is stabilized in a polar medium. Unlike $[Ru(phen/bpy)_2dppz]^{2+}$, **Ir0** emits weakly in water, whereas the luminescence spectra of the other Ir(III) complexes described here are quenched in aqueous medium. Indeed, Figure 3 shows the emission and excitation spectra of **Ir3** in pure organic solvent (MeCN) and in a mixture of MeCN and water (90:10, v/v). The addition of a small amount of protic solvent has a dramatic effect on the emission properties of Ir(III) dppz-derivatized complexes. Such a quenching had already been observed for $[Ru(phen/bpy)_2dppz]^{2+}$. However, the amount of water required for almost 100% quenching efficiency was higher in this latter case.[44]

Electrochemistry. The electrochemical data obtained by cyclic voltammetry in MeCN for each Ir(III) complex are gathered in Table 1. The redox potentials in the excited state, estimated from the overlap of the emission and excitation spectra,[45] are also included. All of the complexes display reversible oxidation and reduction waves (Supporting Information). The similarity between oxidation potentials (metal-based) is striking, and these potentials are significantly more positive than that of $[Ir(ppy)_3]$ (E_{ox} = +1.0 V/NHE)[46] and more negative than that of $[Ir(bpy)_3]^{3+}$ (E_{ox} = +2.17 V/NHE).[47] These oxidation potentials reflect therefore the similarity of the metallic core in the Ir−dppz complexes. The iridium complexes display similar reduction patterns, with a potential close to that of $[Ir(bpy)_3]^{3+}$ (E_{red} = −0.76 V/NHE).[47] The reduction wave of **Ir2** is anodically shifted with respect to that of **Ir0**, whereas it is cathodically shifted for **Ir1** in good agreement with the electron density on the dppz-derivatized ligand.

Iridium Complexes and Polynucleotides: Absorption and Emission in the Presence of Natural and Synthetic Polynucleotides. The excited state of most iridium complexes can be sufficiently oxidizing to photooxidize purine moieties and/or reducing to photoreduce pyrimidine moieties. We have therefore examined whether the photochemical properties of these iridium complexes would yield redox damage in DNA.

UV−Vis Absorption. The binding of metal complexes to natural or synthetic DNA can be easily probed by monitoring the UV−vis absorption changes of the complex in the presence of increasing concentration of the biopolymer.[48,49] In the case of the iridium complexes, the absorption properties are considerably altered upon the addition of the polynucleotide. Figure 4 shows the change in absorption of **Ir3** in the presence of increased concentration of λ DNA in aqueous buffered solution. The changes in absorption for the other iridium complexes are comparable as well as the changes induced with other polynucleotides. However, whereas a significant monotonic hypochromical shift is observed for the high-energy absorption bands around 300 nm, **Ir3** displays a more complicated pattern at the low-energy absorption band as a function of titration. Indeed, two phases are observed in the change of absorption. At low polynucleotide/iridium ratios, an increase in the absorbance

(41) Dedeian, K.; Shi, J.; Forsythe, E.; Morton, D. C.; Zavalij, P. Y. *Inorg. Chem.* **2007**, *46*, 1603−1611.
(42) Ichimura, K.; Kobayashi, T.; King, K. A.; Watts, R. J. *J. Phys. Chem.* **1987**, *91*, 6104−6106.
(43) Finlayson, M. F.; Ford, P. C.; Watts, R. J. *J. Phys. Chem.* **1986**, *90*, 3916−3922.
(44) Olson, E. J. C.; Hu, D.; Hörmann, A.; Jonkman, A. M.; Arkin, M. R.; Stemp, E. D. A.; Barton, J. K.; Barbara, P. F. *J. Am. Chem. Soc.* **1997**, *119*, 11458−11467.
(45) Lai, S. W.; Chan, M. C.; Cheung, T. C.; Peng, S. M.; Che, C. M. *Inorg. Chem.* **1999**, *38*, 4046−4055.
(46) Dedeian, K.; Djurovich, P. I.; Garces, F. O.; Carlson, G.; Watts, R. J. *Inorg. Chem.* **1991**, *30*, 1685−1687.
(47) Kahl, J. L.; Hanck, K. W.; De Armond, M. K. *J. Phys. Chem*, **1978**, *82*, 540−545.
(48) Ortmans, I.; Elias, B.; Kelly, J. M.; Moucheron, C.; Kirsch − De Mesmaeker, A. *Dalton Trans.* **2004**, 668−676.
(49) Hartshorn, R. M.; Barton, J. K. *J. Am. Chem. Soc.* **1992**, *114*, 5919−5925.

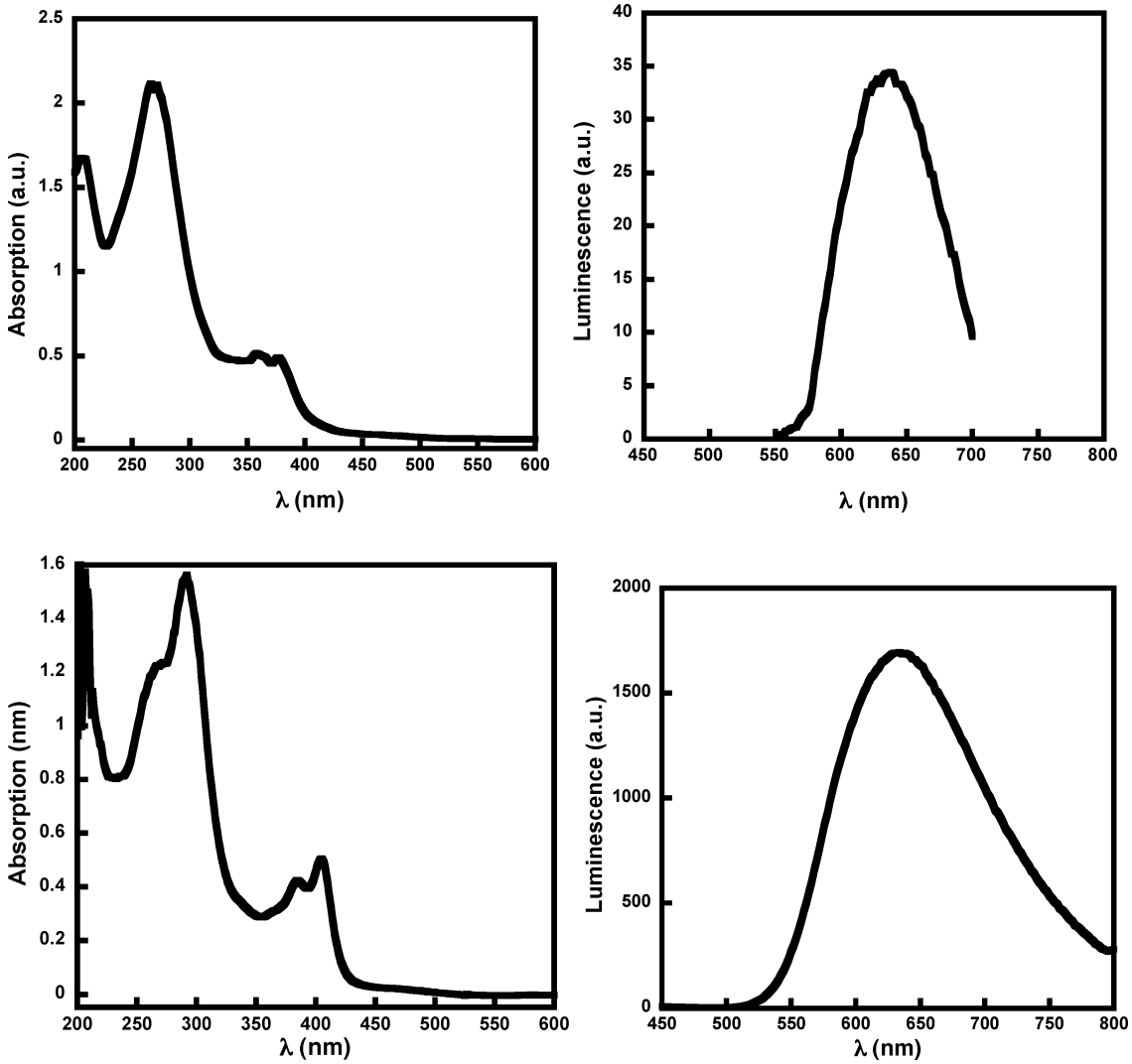

Figure 2. Absorption and emission spectra for Ir(III) complexes. Absorption spectrum of **Ir0** in water (top left, 25 μM) and **Ir3** in acetonitrile (bottom left, 16.5 μM); Emission spectrum of **Ir0** in water (top right, 25 μM) and **Ir3** in dichloromethane (bottom right, 17.6 μM). All of the measurements are made at ambient temperature in air.

is observed. Then, upon further additions of the biopolymer, normal hypochromicity is restored.

Emission. The absence of luminescence of **Ir1**, **Ir2**, and **Ir3** in water is similar to that observed for $[Ru(phen/bpy)_2dppz]^{2+}$ complexes. In this latter case, the luminescence of the complex is restored upon the addition of polynucleotide.[49,50] This light switch-on effect has been attributed to the protection of the luminophore from external sources of nonradiative deactivation when intercalated into the double helix. However, in the case of **Ir1**, **Ir2**, and **Ir3**, neither in the absence nor in the presence of DNA could the luminescence be restored. This result shows that other quenching processes must occur when these derivatized complexes of iridium are bound to DNA.

As **Ir0** luminesces in aqueous solution, the effect of increasing the concentration of different polynucleotides (CT-DNA, CP-DNA, HT-DNA, $[poly(dG\text{-}dC)]_2$, and $[poly(dA\text{-}dT)]_2$) on its emission properties could be monitored under steady-state conditions. The emission spectra as a function of increasing CT-DNA and $[poly(dA\text{-}dT)]_2$ concentrations are shown in Figure 5. Also shown are the relative emission intensities I/I_0 (where I_0 is the emission measured in the absence of polynucleotides) for **Ir0** in the presence of polynucleotides containing different percentage of GC base pairs. Interestingly, luminescence quenching is observed in every case, even when no GC base pairs are present. This quenching process could be attributed to a photoinduced electron-transfer process from one of the bases to the excited iridium complex.

Study by EPR of the Transients Formed under Irradiation of Ir0 in the Presence of $[Poly(dG\text{-}dC)]_2$ and $[Poly(dA\text{-}dT)]_2$. It has previously been shown that the EPR technique can be a useful tool to probe the formation of G radicals.[51] Indeed, upon irradiation of $[Ru(phen)_2dppz]^{2+}$ intercalated into $[poly(dG\text{-}dC)]_2$ in the presence of an external quencher such as $[Ru(NH_3)_6]^{3+}$ or $[Co(NH_3)_5Cl]^{2+}$ (flash−quench technique), the production of a powerful ground-

(50) Hiort, C.; Lincoln, P.; Nordén, B. *J. Am. Chem. Soc.* **1993**, *115*, 3448−3454.

(51) Schiemann, O.; Turro, N. J.; Barton, J. K. *J. Phys. Chem. B* **2000**, *104*, 7214−7220.

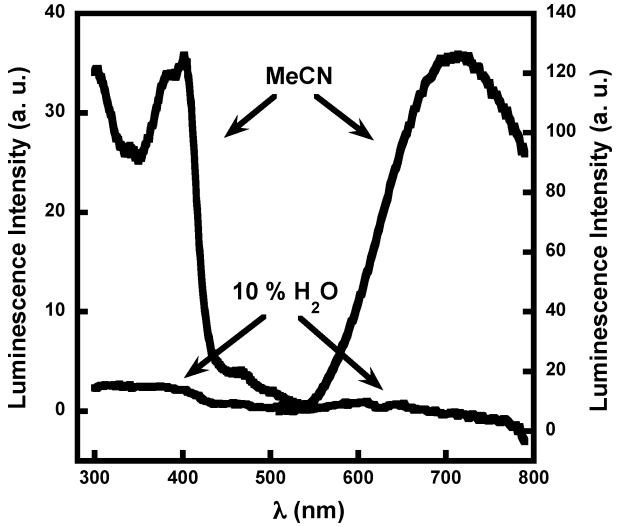

Figure 3. Effect of the addition of 10% of water into MeCN on the emission and excitation spectra of **Ir3**. [Ir3] = 20 μM. The excitation wavelength for the emission spectra is 410 nm, while the excitation spectra are monitored with an emission at 715 nm.

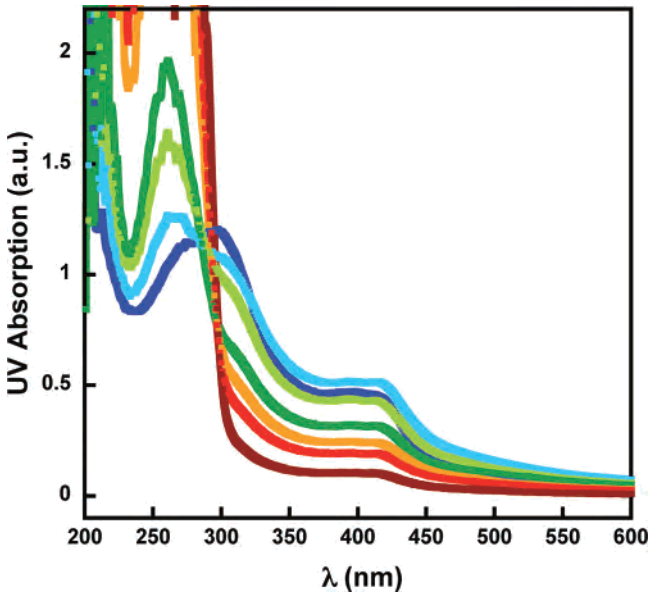

Figure 4. Evolution of the UV−vis absorption spectra of **Ir3** (constant concentration 22 μM) in the presence of increasing concentrations of λ DNA (aqueous buffered solution 10 mM NaCl, 20 mM sodium phosphate pH 7.0). [DNA] = 0 (blue), 50 μM (light blue), 100 μM (light green), 200 μM (green), 405 μM (orange), 540 μM (red), and 609 μM (brown).

state oxidant $[Ru(phen)_2dppz]^{3+}$ leads to the formation of G radicals within the DNA. The guanine radical cation, rapidly deprotonated,[52] reacts in turn very efficiently at ambient temperature with a spin trap for purine radicals, N-*tert*-butyl-α-phenylnitrone (PBN). The so-formed G-PBN entity displays characteristic EPR signals.[51]

To test the occurrence of a photoinduced electron-transfer process between **Ir0** and polynucleotides as suggested from the luminescence data, EPR studies were carried out at ambient temperature in the presence of PBN as a spin-trap. Thus, an aqueous buffered solution (TRIS-HCl, 50 mM, pH 7) of **Ir0** (50 μM) containing $[poly(dG\text{-}dC)]_2$ (1 mM) and PBN (3 mM) was irradiated at ambient temperature for 90 s at $\lambda > 350$ nm. The subsequent EPR spectrum measured in the dark (Figure 6) corresponds closely to that previously reported for the trapping of guanine radical with PBN (g = 2.0059, a_N = 15.50, a_H = 3.21).[51] Importantly, no EPR signal was detected in the absence of irradiation or upon omitting any one of the three reactants, for example, **Ir0**, $[poly(dG\text{-}dC)]_2$ or PBN. Moreover, as expected for the G-PBN entity, the EPR signal is stable for a few hours in the dark. However, upon further irradiation, the intensity of the original EPR signals decreases with a concomitant grow-in of a second signal (data not shown). This observation has already been reported and corresponds to the decomposition of the nitroxide radical in the G-PBN entity upon irradiation.[51]

The same experiment has been conducted in the presence of $[poly(dA\text{-}dT)]_2$ (**Ir0**: 50 μM; $[poly(dA\text{-}dT)]_2$: 1 mM; PBN: 3 mM; aqueous buffered solution TRIS-HCl 50 mM, pH 7; hν for 90 s at $\lambda > 350$ nm). Indeed, the PBN spin-trap is also known to react efficiently with A radicals, if present in the medium.[52,53] Interestingly, no EPR signal was detected in the presence of $[poly(dA\text{-}dT)]_2$ for **Ir0** or **Ir3** (Figure 6). Thus, one-electron oxidation of adenine moieties by the excited state can be excluded.

To test for the formation of guanine radicals in the presence of the derivatized dppz complex, **Ir3** was irradiated in the presence of $[poly(dG\text{-}dC)]_2$ (1 mM) and PBN as a spin-trap (3 mM) under the same irradiation conditions used for **Ir0**. The EPR spectrum (part c of Figure 6) again shows features characteristic of the G-PBN entity. The signal is, however, much less intense than that of **Ir0** under the same conditions. This decrease in intensity may be due to the presence of the linker on the dppz ligand, which would attenuate the interactions between iridium complexes and the base pairs and thus would decrease the efficiency of formation of G radicals under irradiation.

Photoredox Reaction of ^{CP}C and ^{CP}G-Containing DNA with Noncovalently Bound Iridium Complexes. The dppz-derivatized iridium complexes can be anchored to oligonucleotides to test whether they can trigger redox damage at a distance from the anchoring site. In this present work, we have therefore tested whether our Ir(III)-derivatized complexes could first induce DNA redox damages when noncovalently bound to DNA. We have carried out irradiation experiments in the presence of modified oligonucleotides to probe sensitively for redox damage. It has previously been shown that cyclopropylamine-modified guanine or cytosine (^{CP}C or ^{CP}G) are fast kinetic hole and electron traps and efficiently report transient charge occupancy on G or C nucleobases.[14,16,25] These systems are thus excellent candidates to probe the formation of base radicals induced by irradiation of a photooxidant or photoreductant located in the DNA duplex.

Table 2 shows the ^{CP}C- and ^{CP}G-modified oligonucleotides used for the irradiation experiments in the presence of noncovalently bound iridium. The DNA assemblies contain

(52) Steenken, S. *Chem. Rev.* **1989**, *89*, 503−520.

(53) Chen, X. H.; Syrstad, E. A.; Nguyen, M. T.; Gerbaux, P.; Turek, F. *J. Phys. Chem. A* **2004**, *108*, 9283−9293.

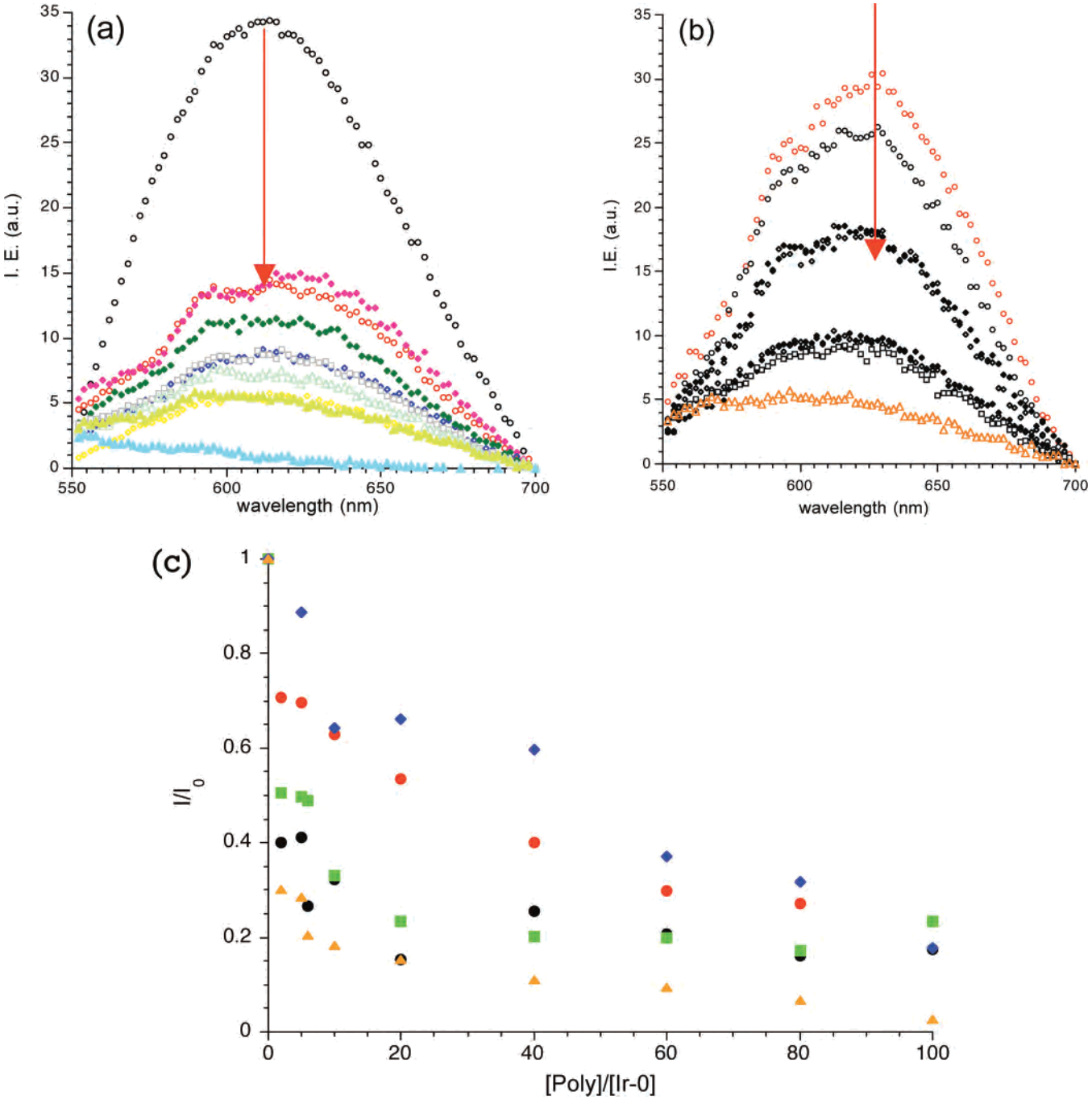

Figure 5. Luminescence quenching of **Ir0** in the presence of increasing concentrations of (a) CT-DNA and (b) $[poly(dA\text{-}dT)]_2$. (c) Change in relative emission intensity for increasing concentration of various polynucleotides containing different percentages of GC base pairs. CT-DNA (black circle) and HT-DNA (green square), 42% GC; CP-DNA (red circle), 26% GC; $[poly(dA\text{-}dT)]_2$ (blue diamond), 0% GC; $[poly(dG\text{-}dC)]_2$ (orange triangle), 100% GC. All of the measurements were made with a constant complex concentration of 10 μM in a 5 mM TRIS-HCl buffered aqueous solution (pH 7).

an A-tract composed of eight AT base pairs. The flanking sequences are random and kept the same to avoid side effects such as fraying ends. After the second adenine base, either a ^{CP}C or ^{CP}G is placed (sequence **I/G**$-^{CP}$**C** and **C**$-^{CP}$**G** respectively in Table 2) as a fast kinetic electron or hole trap. Each strand was irradiated in the presence of **Ir1**, **Ir2**, and **Ir3** ([Ir]: 20 μM; [DNA]: 5 μM 10 mM NaCl, 20 mM sodium phosphate, pH 7; irradiation at 380 nm) and subsequently digested by phosphodiesterase and alkaline phosphatase. The decomposition products were analyzed by RP-HPLC (Experimental Section). Light controls were conducted by irradiating duplexes in the absence of iridium complexes. Decomposition percentages of the ^{CP}C trap in **G**$-^{CP}$**C** or ^{CP}G trap in **C**$-^{CP}$**G** are plotted versus irradiation time for the different derivatized Ir(III) complexes in Figure 7. No undigested or partially digested DNA was evident by HPLC.

Clearly, as illustrated in Figure 7, ^{CP}C and ^{CP}G are decomposed upon irradiation in the presence of the iridium complexes. **Ir1** and **Ir2** induce redox ring-opening of ^{CP}C with similar efficiency upon photoactivation, whereas **Ir3** decomposes it more efficiently. After 20 min of irradiation,

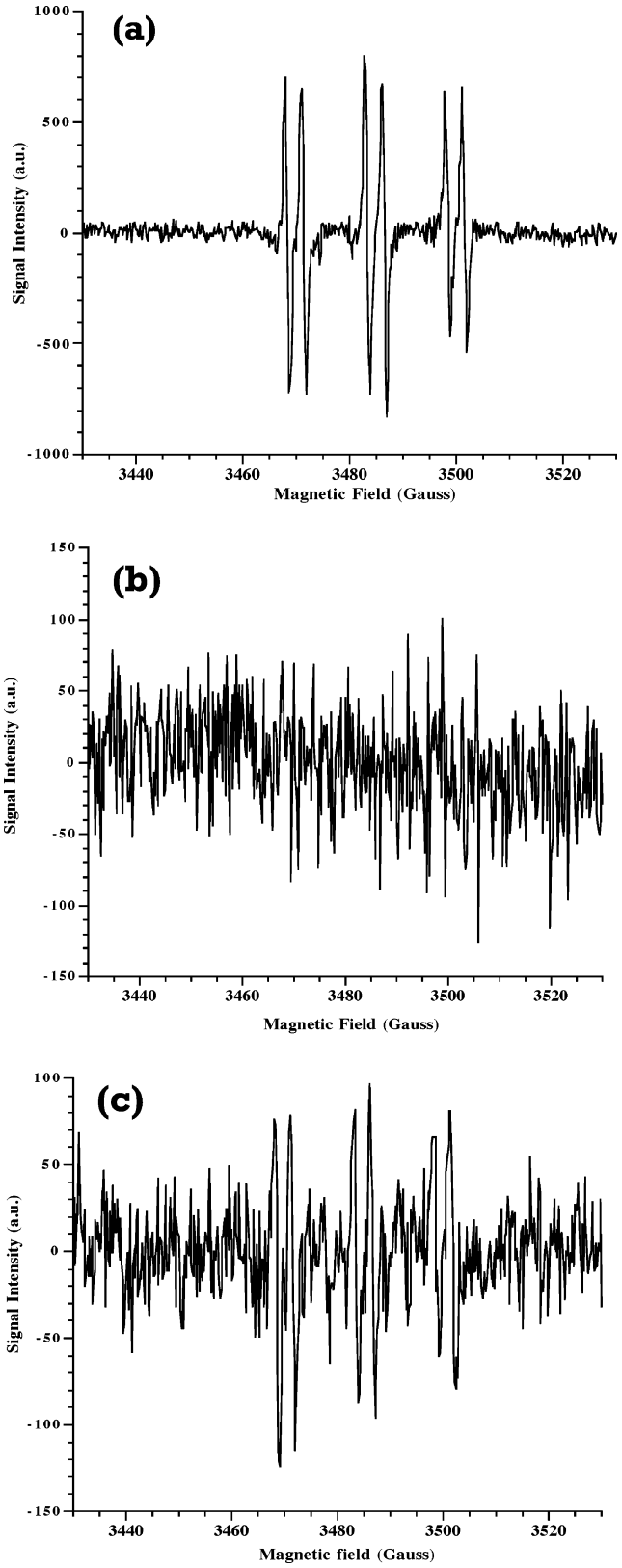

Figure 6. EPR spectra at room temperature for **Ir0** (5×10^{-5} M) in the presence of (a) $[poly(dG\text{-}dC)]_2$ (1 mM) and (b) $[poly(dA\text{-}dT)]_2$ (1 mM) with a spin trap (PBN; 3 mM) after 90s irradiation at $\lambda > 350$ nm. (c) The same with **Ir3** and $[poly(dG\text{-}dC)]_2$. EPR settings: microwave frequency, 9.78 GHz; microwave power, 12.85 mW; number of scans, 4.

51 and 59% of ^{CP}C has been decomposed by **Ir1** and **Ir2**, respectively, whereas a higher value is found with **Ir3** (86%).

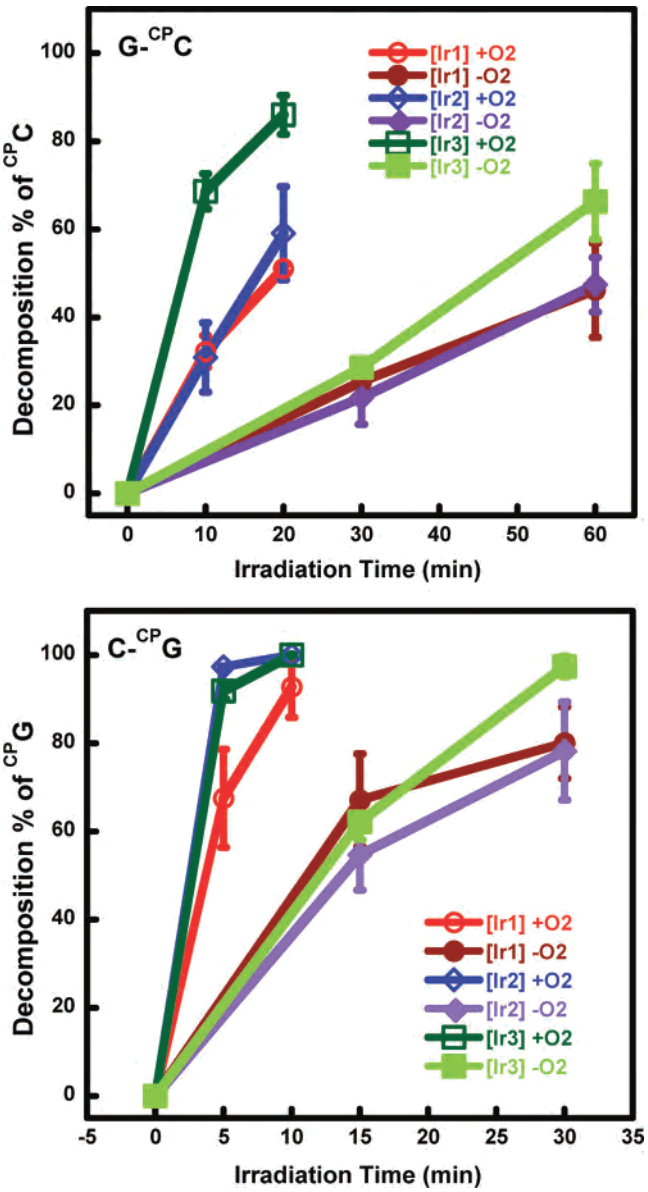

Figure 7. Redox decomposition of ^{CP}C in duplex **G**$-^{CP}$**C** or ^{CP}G in duplex **C**$-^{CP}$**G** upon irradiation in the presence of iridium complexes. Open symbols represent the aerobic data, and close symbols represent the data obtained anaerobically. The concentration of iridium complexes is 20 μM. [DNA] = 5 μM, [NaCl] = 10 mM, and [NaP] = 20 mM. Irradiation wavelength is 380 nm. Top, decomposition data of ^{CP}C; bottom, that of ^{CP}G.

Table 2. Sequences of DNA Assemblies for Irradiation with Noncovalently Bound Iridium Complexes

DNA #	sequences
G$-^{CP}$**C**	5′-ACATT GTTTTTTCAGTCAC-3′ 3′-TGTAA^{CP}CAAAAAAGTCAGTG-5′
I$-^{CP}$**C**	5′-ACATT ITTTTTTCAGTCAC-3′ 3′-TGTAA^{CP}CAAAAAAGTCAGTG-5′
^{CP}**G**	5′-ACATT CTTTTTTCAGTCAC-3′ 3′-TGTAA^{CP}GAAAAAAGTCAGTG-3′

In the case of the ^{CP}G-modified strand, the three complexes have almost equal reaction efficiencies except for **Ir1**, which has a slightly slower reactivity at shorter times.

The same photolysis experiments were also carried out under anaerobic conditions (Figure 7, Table 3). Decomposition of ^{CP}C and ^{CP}G still occurs in the presence of each Ir-

Table 3. Oxidation and Reduction of Cyclopropylamine-Substituted Bases in DNA by Noncovalently Bound Ir(III) Complexes

photoredox reaction[a]			Ir1	Ir2	Ir2
^{CP}C	$+O_2$[b]	Ox[c]	−[e]	+	−
		red[d]	+	±[f]	+
	$-O_2$	Ox/red	+	+	+
^{CP}G	$+O_2$	Ox	+	+	+
	$-O_2$	Ox	+	+	+

[a] Photolysis of Ir(III) complexes with ^{CP}C− and ^{CP}G-containing duplexes. Details are in the Experimental Section. [b] $+O_2$ and $-O_2$ represent the experiments conducted aerobically or anaerobically. [c] Ox represents the oxidation of the cyclopropylamine-substituted bases induced by the photolysis of noncovalently bound Ir(III) complexes. [d] Red represents the reduction of the cyclopropylamine-substituted bases induced by the photolysis of noncovalently bound Ir(III) complexes. [e] − represents no reaction and + represents a positive reaction occurring under the indicated working conditions. [f] ^{CP}C decomposition is observed in both DNA assemblies, **I**−^{CP}**C** and **G**−^{CP}**C**. Neither reduction nor oxidation of ^{CP}C can be excluded.

(III) complex, although with a somewhat lower efficiency. The overall lower efficiency of ^{CP}C and ^{CP}G decomposition under anaerobic conditions likely reflects the poor solubility of the complex in aqueous buffer, as well as under freeze−pump−thaw conditions. It is unlikely to be the result of $^1O_2$ sensitization, given the fact that the luminescence of the complexes is quenched in an aqueous solution.

Effects of Paired Bases on ^{CP}C Decomposition Triggered by Irradiation of Iridium Complexes. To study the base-pair effects on redox decomposition of cyclopropylamine-derivatized cytosine, an identical sequence to **G**−^{CP}**C** in which the ^{CP}C is base-paired with an inosine unit has been synthesized (**I**−^{CP}**C**, Table 2). As a result of the higher oxidation potential of inosine (1.5 V vs NHE)[26] than that of guanine (1.3 V vs NHE),[54] inosine is less competitive as a thermal hole trap than guanine. Indeed, it has been shown previously that when ^{CP}C is photooxidized by Rh(III) complexes, its decomposition when base-paired to inosine is significantly more efficient than when base-paired to guanine.[14] This enhancement has been attributed to the fact that inosine is a less energetically favored thermal hole trap than guanine. In the present case, as shown in Figure 8, no dramatic enhancement of ^{CP}C decomposition in I-containing duplex is observed in the photolysis of noncovalently bound **Ir1** and **Ir3**. **Ir2** triggers the decomposition of ^{CP}C in a somewhat similar way as canonical photooxidants, whereas, unexpectedly, in the case of **Ir3**, ^{CP}C decomposes slightly more efficiently in **G**−^{CP}**C** than in **I**−^{CP}**C**.

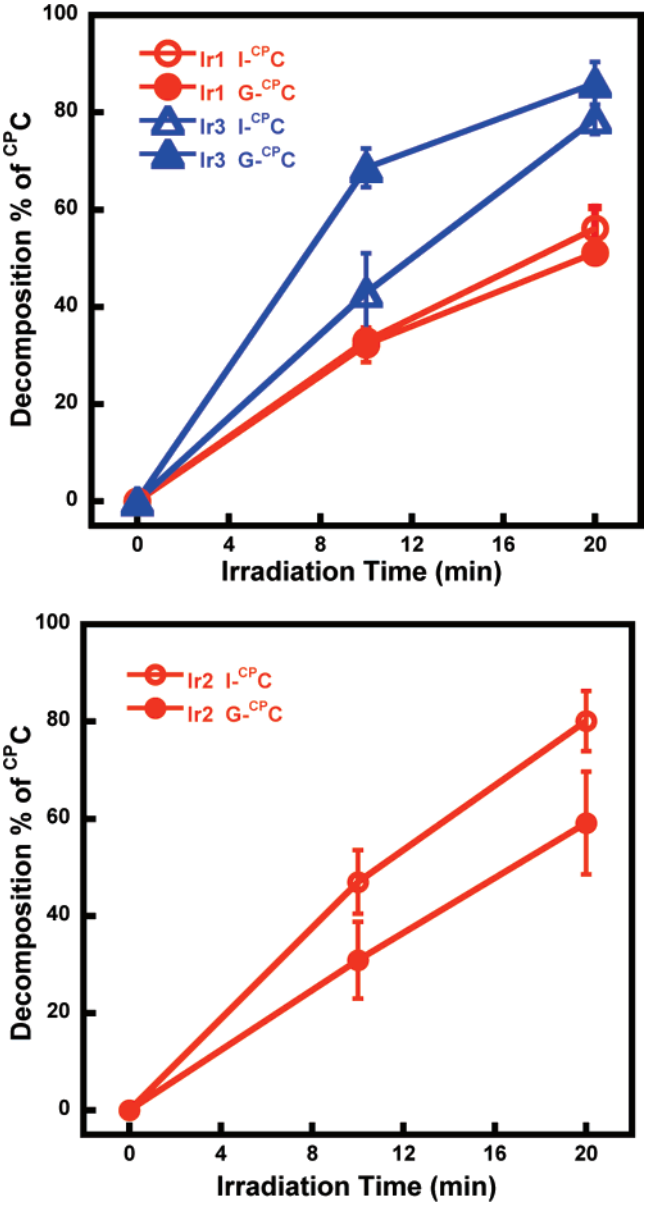

Figure 8. Effects of the paired base on ^{CP}C decomposition triggered by irradiation of iridium complexes. Top: Time course of ^{CP}C decomposition with **Ir1** (red) or **Ir3** (blue). Bottom: Time course of ^{CP}C decomposition with **Ir2** (red). Open symbols represent the data for duplex **I**−^{CP}**C**. Close symbols represent the data for duplex **G**−^{CP}**C.** Experiments were carried out aerobically.

Discussion

Design and Synthesis of Ir(III) Complexes. Iridium chemistry provides a valuable system to develop reactions to trigger hole and electron injection in DNA. Because charge migration along the DNA helix can only be properly studied when the metallic complex is covalently tethered to the phosphate backbone and separated from the electron or hole trap, we have developed Ir(III) complexes with a linker that may be used to anchor the complexes to DNA. Here, the linker is added directly onto the dppz ligand. Using general coupling methods, this can be accomplished readily so that either ether, acyl, or ethynyl-derivatized linkers (**Ir1**, **Ir2**, and **Ir3** respectively) can be introduced at the C_{11} position of the dppz ligand.

Compared to Rh(III) or Ru(II) metal complexes, the third-row metal complexes, and most particularly Ir(III), are characterized by the inertness of their coordination sphere, as evidenced by the somewhat harsh experimental conditions required to substitute the chloride ligands from the starting iridium salts.[55] The addition of the dppz ligand onto the dichloro-bridged iridium precursor is then achieved, and cyclometalated complexes may be obtained.

(54) Steenken, S.; Jovanovic, S. V. *J. Am. Chem. Soc.* **1997**, *119*, 617−618.

(55) Dixon, I. M.; Collin, J.-P.; Sauvage, J.-P.; Flamigni, L.; Encinas, S.; Barigelletti, F. *Chem. Soc. Rev.* **2000**, *29*, 385−391.

Spectroscopy and Electrochemical Properties. Ir(III) complexes are known to display various excited-state properties depending on the ancillary ligands chelated by the Ir(III) center.[42,43,55] When the ligands are negatively charged, the emitting excited state has a high degree of metal-to-ligand charge-transfer (MLCT) character, because the charge compensation induced by the anionic ancillary ligands allows the oxidation of the metal to proceed upon irradiation. In contrast, when the ligands are less σ-donating (like bpy compared to ppy), the excited state is mainly ligand centered because less charge compensation can stabilize the metal core. Thus, in the case of $[Ir(bpy)_3]^{3+}$, the excited state is characterized by a low MLCT percentage (<20∼30%),[56,57] whereas for $[Ir(ppy)_3]^{3+}$ the emission data are consistent with an MLCT excited state.[46] In the present case, for complexes combining two ppy ancillary ligands and one bpy type ligand (dppz), it is likely that the excited state will be mainly MLCT based, as evidenced for other similar mononuclear Ir(III) complexes $[Ir(ppy)_2(HAT)]^+$ (HAT = 1,4,5,8,9,12-hexaazatriphenylene)[40] or $[Ir(ppy)_2(dpp)]^+$ (dpp = 2,3-di(2-pyridyl)-pyrazine).[58] The absorption and emission band shifts of **Ir1**, **Ir2**, and **Ir3** upon either modification of the dppz ligand or change in solvent composition are in agreement with this notion. As with other similar classes of Ir(III) complexes,[55] the electrochemical data show a metal-based oxidation, whereas the reduction is exclusively ligand centered. In our case, it is clear that an electron-withdrawing functional group (in **Ir2**) pushes the reduction potential to more-positive values, and electron-donating groups shift to more-negative values (**Ir1**). The reduction pattern is thus consistent with an electron adding onto the dppz ligand, the reduction of ppy moiety occurring at much more-negative potentials.[46,55] All of the data presented are in agreement with a lowest excited state corresponding to a charge transfer from the iridium metallic center to the dppz ligand, as depicted in eq 1.

$$[Ir(III)(ppy)_2(dppz)]^+ + h\nu \rightarrow [Ir(IV)(ppy)_2(dppz^{\bullet-})]^{*+} \quad (1)$$

This behavior is similar to that observed for $[Ru(bpy)_2(dppz)]^{2+}$, where it is now generally accepted that the lowest emitting state corresponds to a state where the charge is localized on the bpy portion of the dppz ligand. However the situation in this latter case is somewhat much more complicated, because the photophysics is governed by an equilibrium between dark and bright states.[44,59−61] We are currently unable to confirm the presence of a similar process in our Ir(III) complexes, and further spectroscopic investigations are required.

The Ir(III) complexes here show a high oxidizing power and relatively high reducing power in the excited state as evidenced from their E_{red}* and E_{ox}* values (Table 1). On the basis of irreversible redox properties of isolated nucleobases (E_{ox}: 1.3 V for G and 1.4 V for A; E_{red}: −1.1 V for U and T),[54,62] it is not unreasonable to expect at least the oxidation of purines (guanine and adenine) and the reduction of pyrimidines (cytosine and thymine) upon irradiation in the presence of the iridium complexes.

Spectroscopic Behavior in the Presence of Natural and Synthetic DNAs. The changes in absorption resulting from the interaction of iridium and DNA are similar to those previously reported for dppz complexes of Ru(II)[48,49] or Re(I)[63] in the presence of natural or synthetic polynucleotides where the intercalation of the dppz ligand between the bases of DNA is responsible for the variations seen in absorption intensity. The high hypochromicity observed for **Ir3**, for example, in the presence of increasing concentration of polynucleotide has already been evidenced for the $[Pt(mes)_2(dppz)]Cl_2$ complex and the bulky $[Ru(bpy)_2(tpqp)]Cl_2$ (tpqp: 7,8,13,14-tetrahydro-6-phenylquino-[8,7-k][1,8]phenanthroline) complex.[25,64] The observation of an initial hyperchromic shift of the low-energy bands is most likely due to, as suggested with the other complexes, the aggregation of **Ir3** in aqueous solution to protect dppz′ from the solvent molecules. At low DNA concentrations (DNA bp concentration <100 μM), the addition of DNA duplexes disrupts the aggregation of the complex and leads to the enhancement of the absorbance. Once the aggregation is disrupted, and the concentration of DNA is sufficiently high, the normal hypochromic shifts can be observed.

The luminescence quenching observed for **Ir0** in the presence of the increasing concentration of various polynucleotides is similar to that observed for highly oxidizing Ru(II) complexes such as $[Ru(TAP)_2L]^{2+}$ (L = dppz, bpy, phen; TAP = 1,4,5,8-tetraazaphenanthrene).[65] However, in that case, two types of behaviors are observed depending on the GC content of the polynucleotide. Indeed, when no GC base pairs are present, that is, for $[poly(dA\text{-}dT)]_2$, a strong luminescence enhancement is observed. This effect has been attributed to a decrease in the efficiency of the nonradiative deactivation processes of the ^{3}MLCT excited state induced by the double-helix microenvironment and protection from oxygen quenching. In contrast, when polynucleotides containing GC base pairs are added to the complex solution, the emission is quenched. This quenching process has been attributed to a photoinduced electron-transfer process from a guanine moiety to the high-oxidizing triplet excited state of the $[Ru(TAP)_2L]^{2+}$ complex (E_{red}* ≈ +1.4 V/NHE). In our case, the photoreactivity of **Ir0** toward the different natural and synthetic polynucleotides can be rationalized based on the electrochemical properties. Indeed, on the basis

(56) Watts, R. J. *Comments Inorg. Chem.* **1991**, *11*, 303−337.
(57) Demas, J. N.; Harris, E. W.; Flynn, C. M.; Diemente, D. *J. Am. Chem. Soc.* **1975**, *97*, 3838−3839.
(58) Serroni, S.; Juris, A.; Campagna, S.; Venturi, M.; Denti, G.; Balzani, V. *J. Am. Chem. Soc.* **1994**, *116*, 9086−9091.
(59) Olofsson, J.; Onfelt, B.; Lincoln, P. *J. Phys. Chem. A* **2004**, *108*, 4391−4398.
(60) Brennaman, M. K.; Alstrum-Acevedo, J. H.; Fleming, C. N.; Jang, P.; Meyer, T. J.; Papanikolas, J. M. *J. Am. Chem. Soc.* **2002**, *124*, 15094−15098.
(61) Brennaman, M. K.; Meyer, T. J.; Papanikolas, J. M. *J. Phys. Chem. A* **2004**, *108*, 9938−9944.
(62) Steenken, S.; Telo, J. P.; Novais, H. M.; Candeias, L. P. *J. Am. Chem. Soc.* **1992**, *114*, 4701−4709.
(63) Stoeffler, H. D.; Thornton, N. B.; Temkin, S. L.; Shanze, K. S. *J. Am. Chem. Soc.* **1995**, *117*, 7119−7128.
(64) Rüba, E.; Barton, J. K. *Inorg. Chem.* **2004**, *43*, 4570−4578.
(65) Elias, B.; Kirsch − De Mesmaeker, A. *Coord. Chem. Rev.* **2006**, *250*, 1627−1641.

of the reduction potential for the excited state, it seems reasonable that, following irradiation, a reductive quenching of the excited state by the guanine moiety takes place as shown in eq 2.

$$[Ir(IV)(ppy)_2(dppz^{\bullet -})]^{*+} + G \rightarrow [Ir(III)(ppy)_2(dppz^{\bullet -})] + G^{\bullet} + H^{+} \quad (2)$$

This notion is in good agreement with the data obtained by EPR. Indeed, the formation of an adduct between PBN and a guanine radical results from the addition of the nitrone on the C_4 site of the guanine ring (Supporting Information). In the present case, the guanine radicals stem thus from the one-electron photooxidation of a guanine moiety by the excited **Ir0** complex. Very interestingly, irradiation experiments conducted with **Ir0** in the presence of $[poly(dA\text{-}dT)]_2$ and PBN as a spin trap do not lead to any EPR signals, whereas significant luminescence quenching is observed when the complex is irradiated in the presence of the same polynucleotide. As the excited state of **Ir0** might potentially oxidize adenine moieties, the luminescence quenching could originate from a similar photooxidative process as described for guanine. However, if this is true, adenine radical cations should also react with PBN and lead to a significant EPR signal due to the A-PBN entity.[52,53,66] These results support the hypothesis for the need of a different photoinduced process to explain the inhibition of luminescence of **Ir0** upon the addition of $[poly(dA\text{-}dT)]_2$ in the medium. We propose that the quenching originates from a photoreductive process of thymine bases by excited **Ir0** as described in eq 3.

$$[Ir(IV)(ppy)_2(dppz^{\bullet -})]^{*+} + T \rightarrow [Ir(IV)(ppy)_2(dppz)]^{2+} + T^{\bullet -} \quad (3)$$

Studies with Cyclopropylamine-Modified Oligonucleotides. The results outlined above show that both oxidative and reductive damages can be triggered by the dppz complexes of iridium. Taking advantage of the fast ring-opening chemistry of modified bases upon one-electron oxidation or reduction, we have studied the behavior of our modified dppz Ir(III) complexes to give further evidence for the presence of oxidative or reductive damage to DNA under irradiation (Table 3). The fact that ^{CP}G is very efficiently decomposed under irradiation in the presence of all three iridium complexes support the formation of the guanine radical, as described above. In the case of ^{CP}C, it is known that efficient ring opening occurs both under one-electron oxidation or one-electron reduction.[14,25] ^{CP}C oxidation is characterized by a higher efficiency of decomposition when base-paired to an inosine unit instead of a guanine. The enhancement of ^{CP}C decomposition when base-paired to inosine is absent, in the case of the ^{CP}C reduction.[25] Thus, the base-pair effects can be used to discern the redox reactions that cause the ring opening of ^{CP}C. In the case of noncovalently bound **Ir1** or **Ir3** irradiated in the presence of ^{CP}C-containing strands, the lack of I-enhancement effect on ^{CP}C decomposition could indicate that ^{CP}C is photoreduced by the iridium complexes. Thus, both **Ir1** and **Ir3** can only oxidize purines and reduce pyrimidines, upon photoexcitation. For **Ir2**, ^{CP}C is consumed more efficiently when base-paired to inosine. Because **Ir2** has a relatively higher E_{red}^{*} than **Ir1** and **Ir3** (Table 1), it is more likely that photooxidation processes would be the dominant reaction when DNA is irradiated in the presence of this particular iridium complex.

Conclusion

Four cyclometalated Ir(III) complexes containing either functionalized or unfunctionalized dppz ligands have been synthesized and fully characterized. Optical and redox features of the complexes are modulated by the functional group with different electron affinities. The Ir(III) complexes exhibit unique excited-state redox properties and can be applied to trigger both oxidation and reduction of DNA bases. Luminescence and EPR measurements have shown the presence of a photoinduced electron-transfer process leading to guanine oxidation and, as shown indirectly, to thymine reduction.

Redox decomposition of both ^{CP}C and ^{CP}G in a DNA duplex is observed upon the irradiation of the noncovalently bound iridium-derivatized complexes with DNA. Unlike oxidation, ^{CP}C base-paired with guanine is decomposed in a comparable or more efficient way than when base-paired to inosine upon irradiation with **Ir1** or **Ir3**. These results thus provide information on the photochemical behavior of noncovalently bound Ir(III) complexes in the presence of DNA. With monofunctional linkages on the dppz ligand, these iridium complexes can furthermore be covalently tethered to a DNA oligonucleotide, and the resulting Ir−DNA conjugates would possess at the same time a photooxidant and a photoreductant with an identical intercalation mode and electron coupling to DNA.[33] DNA assemblies with **Ir1** or **Ir3** can therefore be remarkably useful to compare the features of ET and HT through the same DNA assembly.

Acknowledgment. We are grateful to the NIH for their financial support. B.E. also thanks the Département des Relations Internationales de l'Université Libre de Bruxelles (Prix Rayonnement International) and the Fondation L. de Bay for postdoctoral fellowships.

Supporting Information Available: Additional absorption, emission spectra, and cyclic voltamograms for Ir(III) complexes. Scheme of reaction between guanine radicals and PBN. This material is available free of charge via the Internet at http://pubs.acs.org.

IC7014012

(66) Bijeire, L.; Elias, B.; Souchard, J.-P.; Gicquel, E.; Moucheron, C.; Kirsch − De Mesmaeker, A.; Vicendo, P. *Biochemistry* **2006**, *45*, 6160−6169.